Science Translational Medicine
AAAS

stm.sciencemag.org/cgi/content/full/12/539/eaay0167/DC1

Supplementary Materials for

Early delivery and prolonged treatment with nimodipine prevents the development of spasticity after spinal cord injury in mice

Maite Marcantoni, Andrea Fuchs, Peter Löw, Dusan Bartsch, Ole Kiehn*, Carmelo Bellardita

*Corresponding author. Email: ole.kiehn@sund.ku.dk

Published 15 April 2020, *Sci. Transl. Med.* **12**, eaay0167 (2020)
DOI: 10.1126/scitranslmed.aay0167

The PDF file includes:

Other Supplementary Material for this manuscript includes the following:

(available at stm.sciencemag.org/cgi/content/full/12/539/eaay0167/DC1)

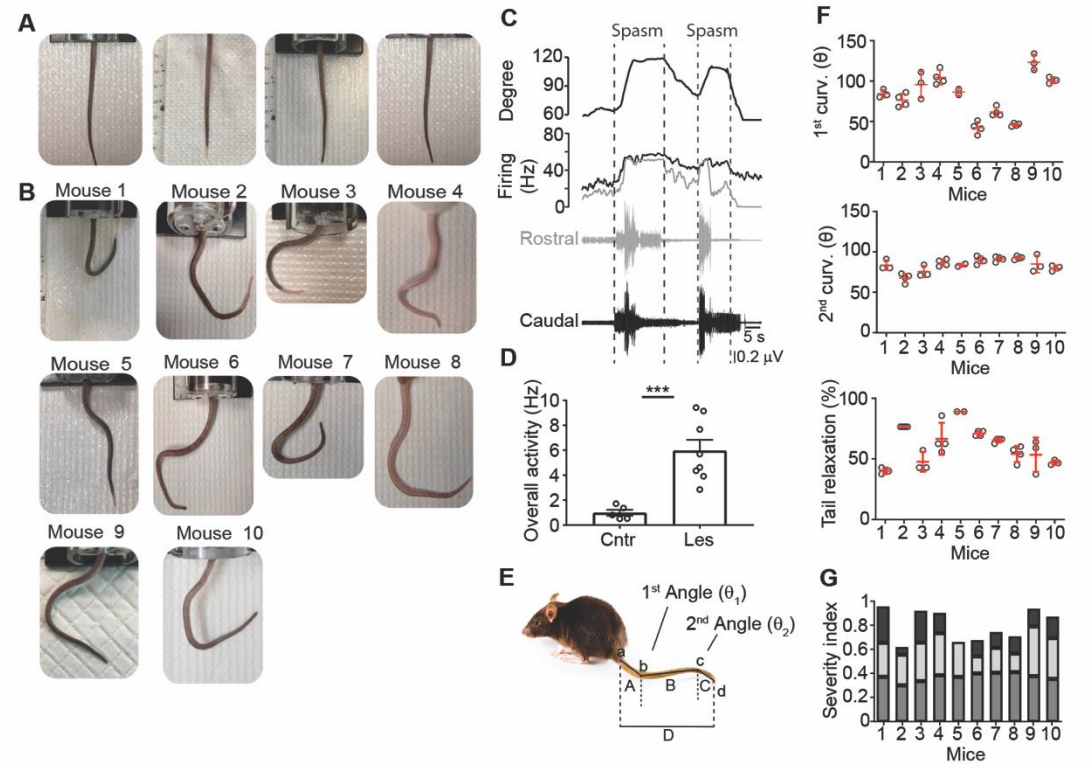

Fig. S1. Tonic muscle contraction and muscle spasms 6 weeks after SCI. A-B. Photographs of tails in wild-type un-lesioned (A) and lesioned mice 6 weeks after SCI (B, N=10). **C.** EMG recordings and firing frequency of rostral (Coccygeal 9th, grey) and distal (Coccygeal 17th, black) muscles with the simultaneous increase in tail curvature in the rostral segment (upper trace, degree) during spontaneous spasms (area in the dashed lines) in a lesioned wild-type mouse 6 weeks after SCI. **D.** Mean firing frequency of motor units of the tail muscles from un-lesioned mice (cntr, motor units=131, N=5) and lesioned mice 6 weeks after SCI (Les, motor units=131, N=8, Welch's *t* test, ***p<0.001). **E.** Schematic of the logic for tail measurements. The tail was divided in 4 points (a-d) and three segments (A-C). The segment D was generated linking the points a and d. **F**. Measurements of first curvature (upper graph), second curvature (middle graph) and relaxation (lower graph) of the tail from the mice depicted in a. **G**. Severity index calculated by weighting the first angle (darkest grey), second angle (dark grey) and relaxation (palest grey). See online methods for a detailed explanation.

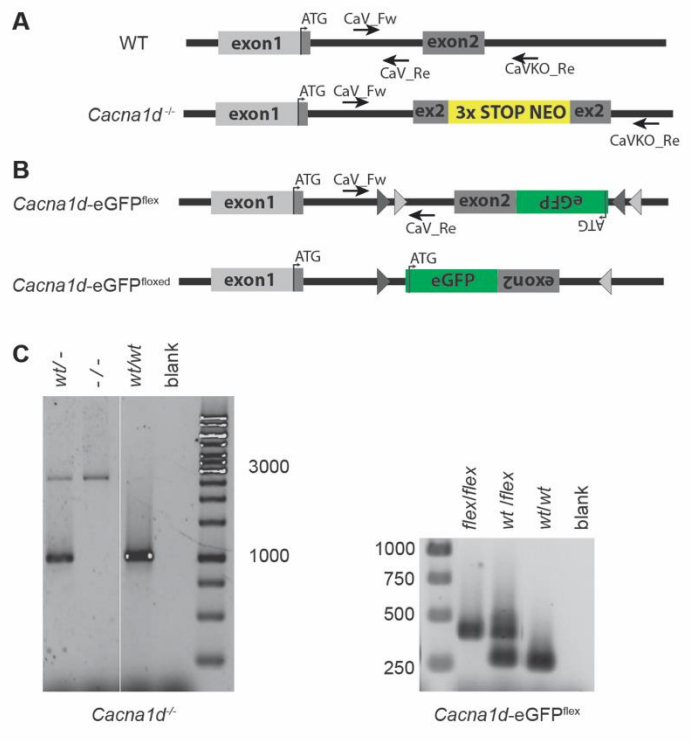

Fig. S2. Genetics of constitutive and the conditional KO *Cacna1d* mice used in the study. A. Schematic of the wild-type allele (WT) and the mutant allele (*Cacna1d*$^{-/-}$) in the targeted area. Homologous recombination produces a truncated α1D subunit resulting in the functional silencing of the Cav 1.3 channels (*Ca$_V$1.3* KO mice). For details see reference 22. **B.** Schematic of the targeting construct (*Cacna1d-eGFP*^{flex}) and the targeted allele after Cre-mediated recombination (*Cacna1d-eGFP*^{floxed}) that results in the expression of the eGFP under the *Cacna1d* promoter and the prevention of *Cacna1d* gene expression. For details see reference 30. **C.** Typical genotyping results showing homo-, heterozygotes and wild type for the constitutive knock out mouse (*Cacna1d*$^{-/-}$, right) and the conditional knock-out (*Cacna1d-eGFP*^{flex}, left). See Material and Methods for more details.

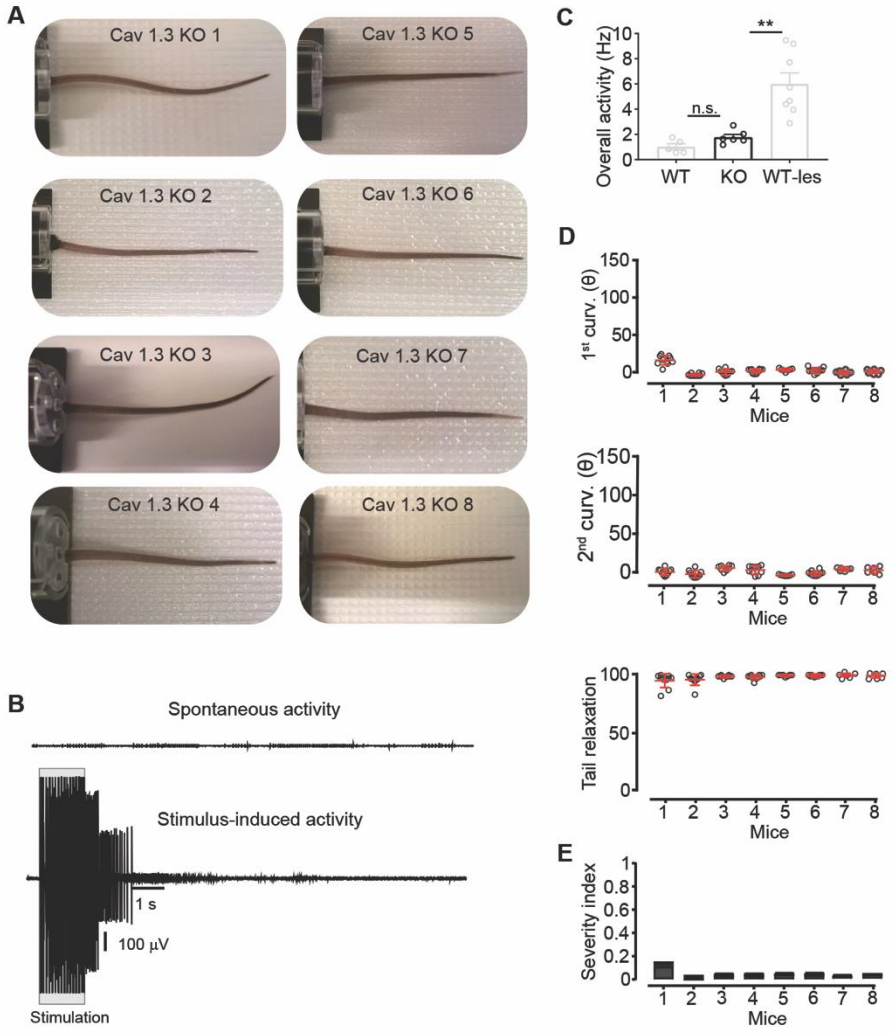

Fig. S3. Tonic muscle contraction and spasms are abolished after SCI in mice with complete silencing of the $Ca_V1.3$ calcium channels. A. Tails of lesioned *$Ca_V1.3^{-/-}$* mice (*Cav1.3* KO, N=8) six weeks after SCI. **B.** EMG recordings from the ventral tail during spontaneous activity at rest (upper trace) and stimulus-induced activity (train of electric stimuli, 500 µs at 10 Hz) in a lesioned *$Ca_V1.3$* KOs mouse. Note that large motor units can be recruited with appropriate stimulation that does not lead to a prolonged spasm. **C.** Overall spontaneous activity from motor units (n=83) from lesioned *$Ca_V1.3$* KO mice (N=8), and un-lesioned and lesioned WT (data are from Figure S1D, Brown-Forsythe and Welch's ANOVA tests followed by Dunnett's multiple comparisons with individual variances computed for each comparison, **p<0.01). **D.** Measurements of first curvature (upper graph), second curvature (middle graph) and relaxation of the tail (lower graph) for the mice depicted in a (mean ± s.e.m. in red). **E**. Severity index of *$Ca_V1.3$* KO mice in D.

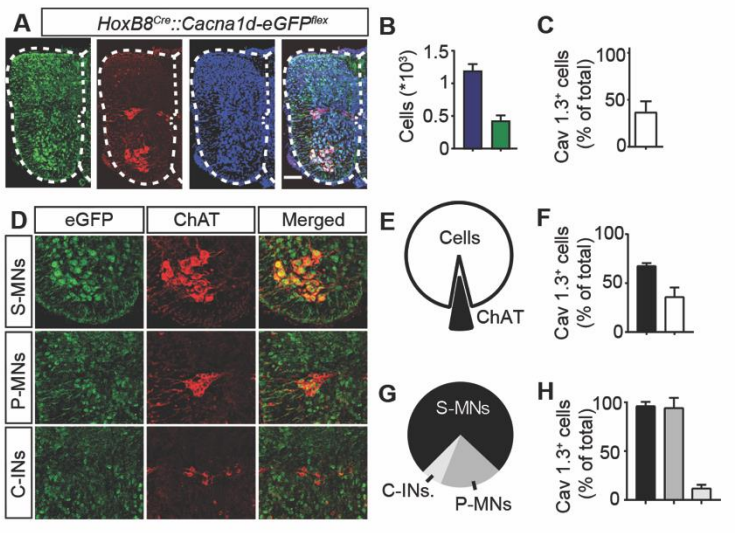

Fig. S4. Expression of $Ca_V1.3$ channels in the spinal cord of newborn mice. A. Confocal images of a transverse section of the spinal cord from a newborn (postnatal day one) *HoxB8^{Cre};Cacna1d-eGFP$^{flex/+}$* mouse stained for eGFP (green), ChAT (red) and Nissl (blue). Scale bar = 100 μm. **B.** Grand mean of spinal cells (Nissl, Blue) and spinal cells expressing Ca_V 1.3 channels ($Ca_V1.3^+$ cells, GFP, green) at the sacral level (n=16, N=4). **C.** Grand mean of Ca_V 1.3^+ cells compared to the total number of spinal cells. **D.** Magnification of confocal images showing the expression of $Ca_V1.3$ channels (eGFP, green) in different cholinergic neurons ($ChAT^+$): somatic motor neurons (S-MNs), preganglionic motor neurons (P-MNs) and cholinergic interneurons (C-INs). **E**. Pie-chart indicating the proportion of $ChAT^+/Ca_V1.3^+$ cells of all Ca_V 1.3^+ spinal cells. **F.** Proportion of $ChAT^+/Ca_V1.3^+$ out of all $ChAT^+$ neurons (black) and proportion of $ChAT^-/Ca_V1.3^+$ cells out of all Nissl stained cells (white). **G.** Proportion of S-MNs (black), P-MNs (dark grey) and C-INs (pale grey) in $ChAT^+$ neurons. **H.** Percent of S-MNs, P-MNs and C-INs expressing $Ca_V1.3$ channels.

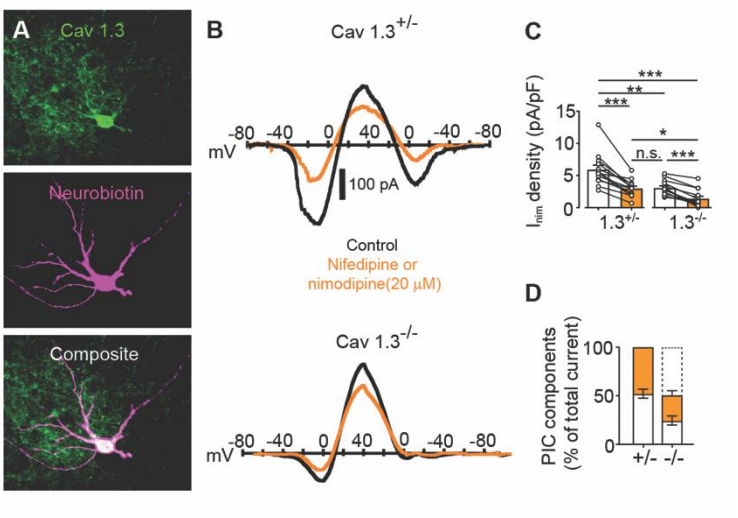

Fig. S5. L-type calcium currents are markedly reduced in neurons of Cav1.3 conditional KO mice. A-B. Representative image of HoxB8-Cav1.3^{+} neuron labeled with biotin and I-V curves in response to voltage-clamp ramps from neurons expressing one copy (*Cav1.3*$^{+/-}$) or no copy of the *Cacna1d* gene (*Cav1.3*$^{-/-}$) in slices from P6-8 mice spinal cords. All recordings were made in the presence of TTX 1 µM, TEA 10 mM and CsCl 25 mM to block sodium and potassium currents. The persistent current (PIC) is seen as a negative slope region in the I-V curves. Black traces are control and orange traces are with nimodipine or nifedipine (dihydropyridine, 20 µM). **C.** Mean current density before and after dihydropyridine (±s.e.m., RM two-way Anova with Geisser-Greenhouse correction, Tukey's multiple comparisons test with individual variances computed for each comparison, n.s.$p>0.05$, *$p<0.05$, **$p<0.01$, ***$p<0.001$). **D**. Different PIC components for all recorded cells: nifedipine sensitive PIC in orange, dihydropyridine insensitive in white, and Cav1.3 current in dashed line. The Cav 1.3 current was estimated by subtraction. Data in C-D are from *Cav1.3*$^{+/-}$ (n=13) and *Cav1.3*$^{-/-}$ (n=13) neurons.